Published in final edited form as:
J Neuroendocrinol. 2012 January ; 24(1): 236–248. doi:10.1111/j.1365-2826.2011.02251.x.

SELECTIVE OESTROGEN RECEPTOR MODULATORS DIFFERENTIALLY POTENTIATE BRAIN MITOCHONDRIAL FUNCTION

Ronald W. Irwin[‡], **Jia Yao**[‡], **Jimmy To**[‡], **Ryan T. Hamilton**[‡], **Enrique Cadenas**[‡], and **Roberta Diaz Brinton**[‡,§,1]

[‡]Department of Pharmacology and Pharmaceutical Sciences, University of Southern California, Pharmaceutical Sciences Center, Los Angeles, California, 90033

[§]Program in Neuroscience, University of Southern California, Los Angeles, California, 90033

Abstract

The mitochondrial energy-transducing capacity of the brain is important for long-term neurological health and is influenced by endocrine hormone responsiveness. This study aimed to determine the role of oestrogen receptor (ER) subtypes in regulating mitochondrial function using selective agonists for ERα (PPT) and ERβ (DPN). Ovariectomised female rats were treated with 17β-oestradiol (E2), PPT, DPN or vehicle control. Both ER selective agonists significantly increased the mitochondrial respiratory control ratio and cytochrome oxidase (COX) activity relative to vehicle. Western blots of purified whole brain mitochondria detected ERα and to a greater extent, ERβ localization. Pre-treatment with DPN, an ERβ agonist, significantly increased ERβ association with mitochondria. In hippocampus, DPN activated mitochondrial DNA-encoded COXI expression whereas PPT was ineffective indicating that mechanistically ERβ, not ERα, activated mitochondrial transcriptional machinery. Both selective ER agonists increased protein expression of nuclear DNA-encoded COXIV suggesting that activation of ERβ or ERα is sufficient. Selective ER agonists up-regulated a panel of bioenergetic enzymes and antioxidant defense proteins. Up-regulated proteins included pyruvate dehydrogenase, ATP synthase, manganese superoxide dismutase, and peroxiredoxin V. *In vitro*, whole cell metabolism was assessed in live primary cultured hippocampal neurons and mixed glia. Results of *in vitro* analyses were consistent with *in vivo* data. Further, lipid peroxides, accumulated as a result of hormone deprivation, were significantly reduced by E2, PPT, and DPN. These findings suggest that activation of both ERα and ERβ are differentially required to potentiate mitochondrial function in brain. As active components in hormone therapy, synthetically designed oestrogens as well as natural phyto-oestrogen cocktails can be tailored to improve brain mitochondrial endpoints.

Keywords

mitochondria; neurone; hippocampus; oestradiol; oestrogen receptor

[1]Address correspondence to: Roberta Diaz Brinton, Ph.D., Department of Pharmacology and Pharmaceutical Sciences, University of Southern California, Pharmaceutical Sciences Center, 1985 Zonal Avenue, Los Angeles, California, 90089, Tel. 323-442-1428; Fax. 323-442-1489; rbrinton@usc.edu.

Author Disclosure Statement: The authors have nothing to declare.

Introduction

Selective oestrogen receptor modulators (SERMs) may serve as therapeutics to mimic the neurotrophic and neuroprotective effects of 17β-oestradiol (E2) without unwanted side effects on reproductive tissues. For women's health, SERMs have the potential to aid the neuroendocrine system during normal aging as the healthy reproductive system is naturally programmed to disengage at menopause. Maintaining a balanced continuum of tissue responsiveness to oestrogens promotes neurological health and general well being.

Previously, we identified bioenergetic-associated changes within the brain mitochondrial proteome following E2 replacement (1). We demonstrated that E2 and progesterone but not medroxyprogesterone acetate sustained and enhanced brain mitochondrial energy-transducing capacity (1–4). Whereas E2 and progesterone increased mitochondrial function alone, in combination progesterone and E2 negated benefits to mitochondrial function (4). Despite decades of scientific effort, the exact benefit of steroid hormone replacement therapy for perimenopausal women remains clinically unclear. Hormone therapy is administered to relieve transient menopausal vasomotor symptoms i.e. hot flushes, night sweats, and associated insomnia (5). Basic neuroscience research firmly holds that gonadal hormones regulate brain metabolic functions to benefit the reproductively fit in a host of animal models (6, 7). Mitochondrial dysfunction manifests well before detectable pathogenic hallmarks of neurodegenerative disorders, including amyloidogenesis and tauopathy in Alzheimer's disease (8, 9). Mitochondrial dysfunction disrupts calcium homeostasis and increases oxidative stress within apoptotic subpopulations of neurones, proposed to underlie neurodegenerative pathologies and associated cognitive decline (10). Bcl-2 expression potentiates the maximal intramitochondrial calcium uptake capacity (11). To prevent apoptosis, mitochondrial calcium load tolerance is increased by E2 in primary cultured hippocampal neurones and isolated rat brain mitochondria (2, 12, 13). Required for E2-induced neuroprotection, E2 induced a rapid protein–protein interaction between an extranuclear oestrogen receptor (ER) and the phosphatidylinositol-3-kinase (PI3K) regulatory subunit p85, to coordinate activation of two membrane-associated signalling pathways, pERK1/2 and pAkt in the same population of neurones. (14). Activated MAPK pERK1/2 subsequently phosphorylates cAMP response element-binding protein (CREB), upregulating gene transcription, including spinophilin (15) and Bcl-2 (13). Further, we have shown that mitochondrial dysfunction precedes Alzheimer's disease pathology and is exacerbated during female reproductive senescence (16, 17).

Oestrogenic molecules regulate metabolic functions by an array of signalling and transcriptional pathways sustaining the energetic demands of neuronal activation (2, 6). ERβ/ERα dimerization can repress ER-responsive promoters on genes that include progesterone receptor and ERα itself by altering the recruitment of c-fos and c-jun coregulator proteins. In the central nervous system, both ERα and ERβ are co-expressed in brain regions that include the preoptic area, the bed nucleus of the stria terminalis, locus ceruleus, and the medial and cortical amygdaloid nuclei. Within the ventromedial hypothalamic nucleus and subfornical organ regions, only ERα was detected (18, 19). In contrast, both *in situ* hybridization histochemistry and immunocytochemistry techniques revealed ERβ expression predominates in the cerebral cortex and in the hippocampus (18, 19). Activation of either or both oestrogen receptors was found to be neuroprotective in primary cultured neurones (20). A phyto-oestrogen combination designed to optimally target ERβ in the brain was shown by Zhao et al. to be neuroprotective with bioenergetic efficacy in the OVX rat model (21) and long-term efficacy in a preclinical mouse model of human menopause (22). The presence of brain mitochondrial oestrogen receptors was proposed and immunocytochemical studies demonstrated mitochondrial ERs by independent laboratories (23–25). Extranuclear ERs have also been shown to functionally bind radiolabelled-E2 in

terminal boutons of the rostral ventrolateral medulla and within the mitochondria of dendritic shafts or synaptic specializations on dendritic spines (26). Through electrophoresis mobility shift assays and surface plasmon resonance Chen and Yager provided evidence *in vitro* that recombinant ERα and ERβ can directly bind mtDNA through interactions with mitochondrial oestrogen response elements and that the binding was increased by E2 (27). Despite the evidence that the ERs are harbored in brain mitochondria, the precise functions and protein isoform identities are still controversial. Increasing the complexity of ER biology, more than 10 splice variants of each ER isoform exist. In the brain, responses to oestrogenic ligands depend on both the presence and the ratio of ER subtypes at the subcellular and anatomical levels. In this study, to determine the differential effects of E2 on metabolic control via mitochondrial function, ovariectomised rats were treated with E2 (steroidal) or non-steroidal selective oestrogen receptor modulators (SERMs). ER-specific ligands were used as pharmacological tools to probe acute ER functions *in vivo* and *in vitro*. The agonist 4,4′,4″-(4-Propyl-[1*H*]-pyrazole-1,3,5-triyl)tris-phenol (propylpyrazoletriol; PPT) is 410-fold more selective for ERα than ERβ and does not act on ERβ transcription whereas 2,3-bis(4-hydroxyphenyl)-propionitrile (diarylpropionitrile; DPN) is 70-fold more selective for ERβ than ERα and has a 170-fold greater relative potency for ERβ in transcriptional assays (28, 29).

The purpose of this study was to distinguish oestrogen receptor subtype initiated pathways in the brain that converge upon mitochondrial function. We propose that in addition to well-established neuroprotective benefits, both ER subtypes would contribute to mitochondrial functional efficiency and reduce oxidative stress. This hypothesis was evaluated in the classical ovariectomised rat model. Our data indicate that activation of either ERα or ERβ differentially rescued the functional efficiency of brain mitochondria, as evidenced by increased electron transport control and reduced oxidative damage.

Materials and Methods

Chemicals

All chemicals were from MP Biomed (Irvine, CA) unless otherwise noted. 17β-oestradiol was obtained from Steraloids (Newport, RI). PPT, 4,4′,4″-(4-propyl-[1H]-pyrazole-1,3,5-triyl)trisphenol (propylpyrazole triol) and DPN, 2,3-bis(4-hydroxyphenyl)propionitrile (diarylpropionitrile) were obtained from Tocris Bioscience (Bristol, UK) (Fig. 1A). For *in vivo* treatments, compounds were dissolved in ethanol and diluted in tocopherol-stripped corn oil with final ethanol concentration <0.001%. For *in vitro* experiments, compounds were dissolved in ethanol and then serial diluted in appropriate cell culture media with final ethanol concentration <0.001%.

Animals and treatments

The Institutional Animal Care and Use Committee (IACUC) at the University of Southern California (Protocol No. 10256) approved the use of animals for the study. Young adult (4–6 month old) female ovariectomised Sprague-Dawley rats purchased from Harlan (Indianapolis, Indiana) were housed under controlled conditions of temperature (22 C), humidity and light (14h light, 10h dark) with water and food available *ad libitum*. After 2 wk of habituation to the facilities and surgery recovery (following ovariectomy), rats were injected subcutaneously with E2 (30 μg/kg), PPT (30 μg/kg), DPN (100 μg/kg) or corn oil vehicle control 24 h prior to sacrifice and forebrain dissection (Fig. 1B). The dose of E2 (30 μg/kg body weight) was chosen as representative of a standard systemic E2 therapy used clinically and in our previous studies (1, 3, 4). A simple mole-to-mole comparison of SERMs was inappropriate since ER binding affinity is greater for PPT (relative binding affinity = 49, scale compared with E2 = 100; 400-fold more selective for ERα) than for DPN

(relative binding affinity 18; 70-fold more selective for ERβ). Based on the E2 (30 μg/kg) dose, we chose PPT (30 μg/kg) and DPN (100 μg/kg), doses that produced brain mitochondrial efficacy. With this same treatment paradigm, our group showed that activation of ERα either by E2 or PPT up-regulated, and DPN down-regulated, hippocampal ApoE mRNA and protein expression (30). At time of sacrifice, uteri were removed and weighed to determine efficacy of E2 treatment (OVX = 0.126 +/− 0.006 g; OVX+E2= *0.285 +/− 0.031 g; OVX+PPT=0.143 +/− 0.010 g; OVX+DPN=0.131 +/− 0.003 g wet weight; n = 5; * $P < 0.05$ vs. OVX) (Fig. 1C). OVX rats were randomised (average body weight 280.6 +/− 2.85 g) to each treatment group and single-housed.

Brain mitochondrial isolation

Brain mitochondria were isolated from rats as previously described (31). Rats were decapitated, and the whole forebrain minus the cerebellum and brain stem was rapidly removed, minced and homogenised at 4°C in mitochondrial isolation buffer [MIB: pH 7.4, containing sucrose (320 mM), EDTA (1 mM), Tris-HCl (10 mM), and Calbiochem's Protease Inhibitor Cocktail Set I (AEBSF-HCl 500 μM, Aprotonin 150 nM, E-64 1 μM, EDTA disodium 500 μM, Leupeptin hemisulphate 1 μM)]. Single forebrain homogenates were then centrifuged at 1,500 × g for 5 min. The pellet was resuspended in MIB, re-homogenised and centrifuged again at 1,500 × g for 5 min. The postnuclear supernatants from both centrifugations were combined and crude mitochondria were pelleted by centrifugation at 21,000 × g for 10 min. The resulting mitochondrial pellet and lipid layer, mostly as a result of myelin, were resuspended in 15% Percoll made in MIB, layered over a pre-formed 23%/40% Percoll discontinuous gradient and centrifuged at 31,000 × g for 10 min. The purified mitochondria were collected at the 23%/40% interface and washed with 10 mL MIB by centrifugation at 16,700 × g for 13 min. The loose pellet was collected and transferred to a microcentrifuge tube and washed in MIB by centrifugation at 9,000 × g for 8 min. The resulting mitochondrial pellet was resuspended in MIB to an approximate concentration of 1 mg/ml. The resulting mitochondrial samples were used immediately for respiratory activity measurements or stored at −80 C for protein, enzymatic, and lipid assays. Previously shown (1), brain mitochondrial purity and integrity of isolated mitochondria with our isolation procedure was confirmed by Western blot analysis for mitochondrial anti-porin (1:500; Mitosciences, Eugene, OR), nuclear anti-histone H1 (1:250; Santa Cruz Biotechnology, Santa Cruz, CA), endoplasmic reticulum anti-calnexin (1:2000; SPA 865, Stressgen, now a subsidiary of Assay Designs, Ann Arbor, MI) and cytoplasmic anti-myelin basic protein (1:500, clone 2, RDI, Concord, MA).

Respiratory measurements

Mitochondrial oxygen consumption was measured polarographically using a Clark-type electrode (Oroboros Instruments, Innsbruck, Austria). One hundred micrograms of isolated mitochondria were placed in the respiration chamber at 37C in respiratory buffer (130 mM KCl, 2 mM KH_2PO_4, 3 mM HEPES, 2 mM $MgCl_2$, 1 mM EGTA) to yield a final concentration of 200 μg/mL. Following 1 min baseline recording, mitochondria were energised by the addition of glutamate (5 mM) and malate (5 mM) as substrates. Stimulated of State 3 respiration was initiated by the addition of ADP (410 μM). State 4 respiration was estimated by the respiration rate following depletion of ADP. The rate of oxygen consumption was calculated based on the slope of the response of isolated mitochondria to the successive administration of substrates. The Respiratory Control Ratio (RCR) was determined by dividing the rate of oxygen consumption/min for state 3 (presence of ADP) by the rate of oxygen consumption/min for state 4 respirations (ADP depleted).

Western blot analysis

Equal amounts of hippocampal protein (20 μg/well) was loaded in each well of a 12% SDS-PAGE gel (Criterion Pre-cast gel; Bio-Rad, Hercules, CA) electrophoresed with a Tris/glycine running buffer, and transferred to a polyvinylidine difluoride membrane (PVDF). The blots were probed with anti-pyruvate dehydrogenase subunit E1α (1:2000; Mitosciences, Eugene, OR), MitoProfile Total OXPHOS Rodent WB Antibody Cocktail consisting of anti-complex I subunit NDUFB8; anti-complex II subunit 30kDa; anti-complex III subunit core II; anti-complex IV COXI; anti-ATP synthase subunit alpha (1:1000; Mitosciences), complex IV COXIV (1:1000; Mitosciences), anti-MnSOD (1:500; BD Biosciences, San Jose, CA), or anti-peroxiredoxin V (1:500; BD Biosciences, San Jose, CA) and the corresponding HRP-conjugated horse anti-mouse or anti-rabbit secondary antibody (Vector; Burlingame, CA) at a concentration of 1:10000. For isolated mitochondria samples, anti-heatshock protein 60 (1:500; BD Biosciences, San Jose, CA) was probed as a loading control. Depending on the molecular weight of probed target proteins, either anti-β-tubulin (1:3000; AbCam, Cambridge, UK) or anti-β-actin (1:3000; AbCam) was used as a loading control for hippocampal lysates. Antigen-antibody complexes were visualised with Pierce SuperSignal Chemiluminescent Substrates (Thermo Scientific) and captured by Molecular Imager ChemiDoc XRS System (Bio-Rad Laboratories). All band intensities were quantified using Un-Scan-it software version 6.1 (Silk Scientific, Orem, UT).

Complex IV/cytochrome c oxidase (COX) activity

Complex IV activity was measured spectrophometrically by monitoring change in absorbance (550nm) of reduced cytochrome c by permeabilised mitochondria (12). Mitochondria were permeabilised in 0.2 mL of 75 mM potassium phosphate buffer (pH 7.5) at 25 C. The reaction was started by the addition of 0.05 mL of 5% cytochrome c previously reduced with sodium hydrosulphite. Cytochrome c oxidase activity was calculated in nanomoles of oxidised cytochrome c per minute per mg protein and reported as rate relative to the mean rate from vehicle control-treated OVX rats.

Lipid peroxidation

Accumulated lipid peroxides in purified brain mitochondria were measured using the leucomethylene blue assay. *t*-Butyl hydroperoxide was used as a standard. Leucomethylene blue was measured by monitoring absorbance at 650 nm after 1 hr incubation at RT. Data values were plotted as pmol/μg protein.

Seahorse XF-24 metabolic flux analysis

Primary hippocampal neurones or mixed glia from day 18 (E18) embryos of timed-pregnant Sprague-Dawley rats were cultured on Seahorse XF-24 (Seahorse Bioscience, Billerica, MA) plates at a density of 75,000 cells per well. Neurones were grown in Neurobasal Medium and B27 supplement for 10 days prior to experiment. Twenty-four hours prior to the experiment cultured neurones were treated with either vehicle, E2 (10 ng/ml; 37 nM), PPT (100 ng/ml; 275 nM), or DPN (100 ng/ml; 420 nM). Mixed glial cells were grown in phenol-red-free DMEM with 10% serum and plated one day prior to treatment. Glial cells were serum starved 4 h prior to treatment. On the day of metabolic flux analysis, both cell cultures were changed to unbuffered DMEM (DMEM base medium supplemented with 25 mM glucose, 1 mM sodium pyruvate, 31 mM NaCl, 2 mM GlutaMax, pH 7.4) and incubated at 37 C in a CO_2-free incubator for 1 h. All media and injection reagents were adjusted to pH 7.4 on the day of assay. Four baseline measurements of Oxygen Consumption Rate (OCR) in pmol/min were taken before sequential injection of mitochondrial inhibitors. Four readings were taken after each addition of mitochondrial inhibitor and prior to automated injection of the subsequent inhibitor. The mitochondrial

inhibitors were added sequentially: oligomycin (1 μM) to inhibit ATP synthase, FCCP (1 μM) to uncouple mitochondria, and rotenone (1 μM) to inhibit Complex I of the ETC. OCR values were presented as OCR percent of baseline to inhibition of ADP-phosphorylation driven respiration. Upon addition of the uncoupling agent, maximum respiratory reserve capacity, a pure estimate of electron transport chain function, reflects how a system reacts to an increased ATP demand. OCR was automatically calculated, recorded, and plotted by the Seahorse XF-24 software.

Oestrogen receptor (ER) protein expression

Western blot analysis of ER was performed using anti-ERβ, PA1-310b (Affinity Bioreagents, now a subsidiary of Thermo Fisher Scientific, Rockford, IL; immunogen: C-terminal amino acids 467–485), an antibody verified by other groups (32, 33). In addition, anti-ERβ H-150 (1:1000; Santa Cruz Biotechnology; immunogen: amino acids 1–150 of N-terminus) was tested as this antibody has been used to identify mitochondrial immunoreactivity in rat primary neurones and the mouse-derived clonal hippocampal cell line HT22 (25) although the specificity of the H-150 antibody has been scrutinised. As an alternative to H-150, the ERβ antibody PA1-310b was recommended based on a comparative study by Sheldahl et al. (33). Anti-ERα, clone 6F11, (1:50; Novacastra, Newcastle Upon Tyne, UK), raised to full length ERα human antigen was used to detect ERα protein expression. Equal amounts of purified mitochondrial protein (20 μg/well) was loaded in each well of a 12% SDS-PAGE gel (Criterion Pre-cast gel; Bio-Rad, Hercules, CA), electrophoresed with a Tris/glycine running buffer, and transferred to a polyvinylidine difluoride membrane (PVDF). Rat ovary homogenate, 10 μg, was used as a positive control for both ERα and ERβ immunoreactivity.

Statistics

Data are presented as means ± SEM and where indicated as percent change relative to OVX. Statistically significant differences were determined by one-way ANOVA followed by Student-Newman Keuls post hoc analysis when appropriate. A $P < 0.05$ was considered statistically significant.

Results

SERMs and 17β-oestradiol enhanced brain mitochondrial respiratory activity

To determine oestrogenic regulation of brain mitochondrial respiration, young adult female Sprague-Dawley rats were ovariectomised to remove endogenous sources of ovarian hormones. The animals were allowed to recover from surgery for 2 weeks to allow for clearance of residual ovarian hormones and to equilibrate to the state of ovarian deprivation. Ovariectomised rats were injected subcutaneously with 30 μg/kg of E2, 30 μg/kg of PPT, or 100 μg/kg of DPN each or equivalent volume of sesame oil vehicle as a control (Fig. 1B). Rats were sacrificed 24 hr later uteri were removed and weighed to confirm oestrogenic response (Fig. 1C) and whole brain mitochondria were isolated. We first measured the respiratory rate of the freshly isolated whole brain mitochondria using glutamate (5 mM) and malate (5 mM) as respiratory substrates. ADP addition to the mitochondrial suspension initiated state 3 respiration. Depletion of ADP was measured as an estimate of state 4 respiration, limited by proton permeability of the inner membrane. There was a significant increase in the respiratory control ratio (RCR) in the PPT, DPN, and E2-treatment groups (Figure 2). *In vivo* pretreatment and subsequent isolation of rat brain mitochondria resulted in increased RCR values of 25% in E2-replaced rats or 15–20% respectively with PPT or DPN compared to vehicle control. Due to limitations of the single-chamber oxygen electrode technique and time-sensitive *ex vivo* mitochondrial preparations, it was not feasible to run dose responses with this measurement. However, previous studies both *in*

vivo and *in vitro* indicated that the positive control E2 dose is within the range of comparison to high physiological level of E2 during the peak of the estrous cycle. At the dose administered both SERMs tested did not induce significant uterine proliferation. The PPT dose used in this study did not cause an increase in uterine proliferation, in a previously dose response study, XXX. PPT and DPN both displayed comparable increases in RCR. We demonstrated that there is an increase in the efficiency of mitochondrial respiration with E2, PPT, or DPN rather than an alteration in the coupling of the electron transport chain.

Pyruvate dehydrogenase and Complex I, II, and III are differentially regulated by oestrogenic treatments

Pyruvate dehydrogenase (PDH) subunit E1α, a component of the key enzyme linking glycolysis to the tricarboxylic acid cycle, was up-regulated 65% by PPT compared to OVX (Fig. 3A) indicating that ERα activation can regulate PDH protein expression within the hippocampus. The ERβ agonist DPN failed to significantly increase expression of PDH despite an average increase of 110% as the variability of PDH expression was high. Three nucDNA-encoded proteins of the electron transport chain complexes I, II, and III respectively were probed within the same Western blot as described in Materials and Methods. Complex I subunit NDUFB8 protein expression was increased by E2 treatment, 23% above OVX expression (Fig. 3B). Complex II subunit SDHB, also a component of succinate dehydrogenase of the glycolytic pathway, was unchanged by all oestrogenic treatments indicating that this protein is not regulated by ER-associated mechanisms (Fig. 3C). Complex III subunit core II protein was equally up-regulated by ~40% following all three oestrogenic treatments suggesting a common activation pathway (Fig. 3D).

Enhanced cytochrome c oxidase (COX) activity and protein expression by oestrogenic treatments

The mitochondrial respiratory chain protein cytochrome oxidase (complex IV) was assayed for activity. COX activity was significantly increased across all treatments equally (Fig. 4). All three oestrogenic treatments displayed a 55% increase in COX activity as compared to OVX. COXI and COXIV protein expression amounts were differentially increased by E2 and SERM treatments *in vivo* (Fig. 3E and 3F). Importantly, in the hippocampus, following 24 h DPN treatment, mtDNA-encoded COXI protein expression was increased by 130% (*i.e.* by 2.3 fold) over the vehicle-treated group. In contrast, PPT had no effect on COXI protein expression indicating that only ERβ, not ERα influenced mtDNA-encoded gene expression. A nucDNA-encoded protein subunit of the same enzyme complex, COXIV was up-regulated by 110%, 107%, 55% following E2, PPT, and DPN oestrogenic treatments respectively, indicating that ERα and ERβ are independently capable of up-regulating specific mitochondrial proteins.

Enhanced Complex V expression

Efficient energy transduction including movement of electrons down the electron transport chain as evidenced by Fig. 2 and Fig. 3 should be coupled to increased ATP production. To determine if ATP synthase/complex V is up-regulated to further accommodate increased energy transduction, we assessed protein expression of complex V, subunit α by Western blot analysis. Complex V, subunit α was increased by 48% and 28% in the respective E2 and PPT treatment groups (Fig. 3G) suggesting this protein is ERα-regulated.

SERMs and 17β-oestradiol alter the antioxidant profile of brain mitochondria

We previously observed effects on H_2O_2 production and a pronounced reduction in lipid peroxidation in the E2-treatment group (3, 4). This would indicate activation of mechanisms beyond solely mitochondrial efficiency in response to E2 that may not be activated in

response to SERMs. Thus we determined the impact of SERMs on the protein expression of the mitochondrial antioxidant proteins MnSOD and peroxiredoxin V (Fig. 6A and 6B) and lipid peroxidation (Fig. 7). MnSOD is responsible for the dismutation of superoxide anion to H_2O_2 and peroxiredoxin V is involved in clearance of H_2O_2 and prevention of peroxidative damage. There was an increase in MnSOD expression of ~25% in the E2 group (Fig. 6A) as compared to OVX. However, PPT and DPN separately had minimal effect, not reaching statistical significance. The expression of peroxiredoxin V was increased by 30% in both the E2- and DPN-treatment groups (Fig. 6B) as compared to control. Results suggest that these antioxidant proteins are up-regulated by oestrogens to prevent further oxidative damage attributed to ovarian hormone deprivation.

SERMs and 17β-oestradiol reduced lipid peroxidation of brain mitochondria

Results of these analyses indicated that brain mitochondrial lipid peroxidation was significantly cleared in ovarian hormone-deprived rats treated acutely with SERMs and E2 compared to vehicle control OVX rats (Fig. 6). When assessed as percent change in lipid peroxides, there was a reduction in mitochondrial lipid peroxidation of ~40%, 65%, and 30% in E2, PPT, and DPN groups, respectively (Fig. 6). Activation of either oestrogen receptor subtype ERα or ERβ was able to elicit a reduction of mitochondrial lipid peroxides. PPT most potently reduced lipid peroxide levels by 65% versus OVX, and 45% compared to DPN, at the dose used (Fig. 6), suggesting that activation of ERα promotes elimination of lipid peroxides in the brain mitochondria. E2 with equal affinity for each receptor and DPN, an ERβ agonist, were also able to significantly reduce lipid peroxides (OVX, 0.1617+/−0.0065 pmol/μg; E2, *0.0931+/−0.0042 pmol/μg; PPT, *0.0579+/−0.0037 pmol/μg; DPN, *0.1066+/−0.0087 pmol/μg protein; * $P < 0.05$ vs. OVX; $n = 4–5$) in purified brain mitochondrial samples from OVX rats treated 24 h prior to tissue isolation.

SERMs and 17β-oestradiol potentiated hippocampal neurone and glia mitochondrial respiratory reserve capacity in vitro

Oxygen consumption rate (OCR) measured in pmol O_2/min was determined using Seahorse XF-24 Metabolic Flux Analyzer as described in the Materials and Methods section. These results from isolated neurones and glia *in vitro* follow the same trend as the results obtained from whole brain mitochondria (Fig. 2) wherein comparable to E2 treatment, both PPT-and DPN-treated neurones elicited increased respiratory responses versus vehicle. As demonstrated previously (3, 16), basal respiration of mixed glia was considerably lower overall than neuronal cultures, reflecting the expected cell type differences in oxygen demand, substrate utilization, and energy transducing capacity. The maximum respiratory reserve capacity, a pure estimate of electron transport chain function, reflects how a system reacts to an increased ATP demand. Following addition of the uncoupler FCCP, both PPT and DPN significantly increased maximal respiratory reserve capacity in both neuronal (Fig. 7A) and glial cultures (Fig. 7B) to OCR comparable to E2 treatment.

Detection of ERα and ERβ in purified brain mitochondria and ERβ expression pattern changes in hippocampus and association with whole brain mitochondria following oestrogenic treatment

The impact of SERMs on hippocampal ERβ (ERβ1; 55 kD) expression was determined by Western blot analysis (Fig. 8A). As a positive control we found an expected decrease in hippocampal ERβ of 46% following E2 treatment. PPT did not significantly reduce ERβ compared to OVX. Interestingly, DPN negatively regulated ERβ, with a 50% decline in expression.

Existence of brain mitochondrial ERα and ERβ was verified by Western blot of OVX rat brain mitochondria. Crude cytosolic and crude mitochondrial fractions from organelle

isolation procedure demonstrated immunoreactivity of both ER subtypes to highly purified mitochondria (Fig. 8B). Blots were intentionally overexposed to demonstrate that non-specific protein (or perhaps other splice variants) immunoreactivity is diminished as purity of fractions increased. ERα (67 kD) was detectable by the monoclonal antibody 6F11. ERβ was detected as variants ERβ1 (55 kD), and ERβ2 (62 kD), concentrated as distinct immunoreactive bands in the mitochondrial fraction. Proteins extracted from rat ovary lysate confirmed ER antibody binding specificity and verified the ER molecular sizes estimated with molecular weight markers in a separate lane. Representative expression of mitochondrial-associated ERα (67 kD) was detected with 6F11 antibody (Fig. 8C, not quantified) but could be attributed to mitochondria of cerebral blood vessels as reported by another group (24, 34). Antibody H-150 detected mitochondrial-associated ERβ1 (55 kD), and ERβ2 (62 kD) immunoreactivity determined by Western blot (Fig. 8C, not quantified). Brain mitochondrial expression of ERβ1 (55 kD; antibody PA1-310b) was quantified. E2 and PPT induced modest 20% increases in ERβ expression/localization relative to OVX. Significantly different from all other groups, DPN-treatment induced a robust 40% increase in ERβ expression/localization relative to OVX brain mitochondria (Fig. 8D).

Discussion

Brain mitochondria from ERα and ERβ SERM-treated rats independently displayed enhanced functional efficiency and increased metabolic rates relative to vehicle control. ERα is the major regulator of estrogen function in the uterus. Increased uterine weight in immature female mice (35) and OVX rats (36) following 4 daily doses of approximately 1 mg/kg PPT and DPN having no uterotrophic response, was able to antagonize PPT uterotrophic responses when treated in combination (35). Our point is that the dose we used, PPT 30 μg/kg, was chosen because it did not elicit a significant uterine increase yet was efficacious for brain mitochondrial function. This is of therapeutic relevance; an ideal neuroSERM would not elicit uterotrophic effects.

Hippocampus, critical for learning and memory functions, was isolated to determine brain-region specific effects of SERM treatment. Results of these analyses indicate that both PPT and DPN significantly increased mitochondrial respiration 24 h following a single *in vivo* exposure. Consistent with an increase in oxidative respiration, PPT and DPN significantly increased electron transport chain complex IV COX enzyme activity in brain mitochondria. And consistent with antioxidant defense from free radicals, E2-, PPT-, and DPN-potentiated respiration was coupled to the reduction of lipid peroxides representing a systematic enhancement of brain mitochondrial efficiency. Underlying this metabolic control is an interpretation of cellular signalling events integrated by ERα- and ERβ-mediated responses converging upon mitochondrial function (37). The data further indicated that PPT and DPN directly and independently regulated mitochondrial function, often with convergent results including enhanced mitochondrial respiration, increased COX activity, and rapid elimination of excess lipid peroxides. The composite mitochondrial outcome profiles compared between E2 and SERMs suggest convergent ER-activated mechanisms such as activation of common signalling cascades to influence mitochondrial function. The precise mechanisms of ERα and ERβ that coordinate the responses are as yet unknown but likely are uniquely regulated by cell types and brain regions that harbor different ratios of ERs, opening therapeutic development opportunities. Together, these data indicate that the oestrogen receptors, activated by SERMs are potent regulators of mitochondrial function to increase both the magnitude and efficiency of mitochondrial respiration in brain.

In the current study, we demonstrated that complex IV activity is significantly increased in response to activation of either ER-subtype. The regulation of COX is of further interest from a transcriptional vantage point due to it being encoded by a combination of

mitochondrial and nuclear genes that must be coordinately expressed. The catalytic core of the multimeric COX holoenzyme comprises the two subunits COXI and COXII and is stabilised by a third subunit, COXIII, all three of which are encoded by mtDNA. Of the thirteen different subunits of COX, ten additional subunits, including COXIV, are encoded by the nuclear genome and are required to fully assemble a functional COX holoenzyme. Corresponding to COX activity, we found changes in COXI and COXIV hippocampal protein expression in the E2 and SERM groups. These results are consistent with our previously reported oestrogenic effects on rodent brain COX activity and expression (1, 3, 4, 16). The COX subunit expression data suggest that activation of either or both ER subtypes is sufficient to increase COX activity. A major difference found in this study was that specifically ERβ directly or indirectly promotes mtDNA-transcribed subunit expression of COXI and possibly other mtDNA encoded subunits. Also based on the data, activation of either or both ERs conferred up-regulation of nucDNA-transcribed COXIV and other critical mitochondrial proteins.

As electrons pass through the mitochondrial electron transport chain, electron leak occurs following formation of the superoxide radical, which is dismutated by MnSOD to form hydrogen peroxide. The hydrogen peroxide can in turn be reduced to water by peroxidases such as glutathione peroxidase or peroxiredoxins. A lack of sufficient peroxidase activity results in the peroxidation of lipids and proteins. Non-specific oxidation of polyunsaturated fatty acids in cellular membranes results in lipid peroxidation, a radical-mediated pathway that generates detrimental degradation products and alters the structure and function of the membrane. Our results demonstrated that SERM treatment cleared lipid peroxides of whole brain mitochondria consistent with our previous studies with E2 (3, 4). The reduction in accumulated lipid peroxides is correlated with oestrogenic increases in expression of MnSOD and PrdxV and interactions with the glutathione system. This E2- and SERM-induced reduction in lipid peroxidation is due to a clearance of accumulated lipid peroxidation induced by 2-week steroid deprivation following ovariectomy in which we previously observed a 30% induction of lipid peroxidation in the OVX compared to ovary-intact rats (3). Activation of brain ERs could up-regulate phospholipid hydroperoxide glutathione peroxidase, which possesses the unique ability to eliminate lipid peroxides (38) and this enzyme was shown to be up-regulated by E2 (39). PPT potently reduced lipid peroxide levels by 65% versus OVX, and 45% compared to DPN, at the dose used, suggesting that activation of ERα is the primary ER-initiated pathway for elimination of lipid peroxides in the brain mitochondria.

Respiratory control is crucial for the maintenance of the metabolic activity network and energy production in which mitochondrial redox potential is coupled with cytosolic signalling. This tightly coupled network integrates various signals to determine cell fate based upon ATP levels, extracellular signals, and energetic demands. Approximately 90% of cellular oxygen is consumed by mitochondrial respiration with the remaining 10% consumed by nonmitochondrial respiration, including substrate oxidation and cell surface oxygen consumption (40, 41). *In vitro*, SERMs potentiated mitochondrial bioenergetics, measured by oxygen consumption rates in neurones and mixed glia cultures. SERMs increased maximal neuronal mitochondrial respiratory capacity indicating that ERα or ERβ activate convergent cellular processes to increase the respiratory capacity of mitochondria necessary for bioenergetically demanding functions such as increased synaptic transmission. In mixed glia, E2 increased both basal and maximal respiratory capacity. Glial cells generate bioenergetic substrates for both neurones and their own energetic demands, the increase in basal respiration is likely due to E2-induced up-regulation of glycolytic pathways as well as maintenance of ion gradients. The results indicated that activation of ERα or ERβ is sufficient to potentiate the maximal mitochondrial respiratory capacity of neurones while simultaneously increasing the capacity of glia to respond to increased demands for

metabolic substrates when required for highly active neural networks. Homeostasis of the glutamatergic system is critical during E2 enhancement of long-term potentiation (2, 6). Assessment of mitochondrial function *in vitro* further verified the responses measured in whole brain purified mitochondria and hippocampal lysates.

In summary, we investigated oestrogenic control of mitochondrial function in the brain and the role of ER-subtypes using SERMs and compared results to the mixed agonist E2. In addition to neuroprotective effects of SERMs (12, 20) and regulation of apolipoprotein E (30), we have now demonstrated that independent stimulation of either ERα or ERβ results in enhanced mitochondrial energy-transducing capacity through balanced respiration and reduced oxidative damage with a single acute dose. SERMs potently enhanced the functional efficiency of whole brain mitochondria as evidenced by up-regulation of critical proteins of glycolytic and oxidative phosphorylation systems. Increased respiratory control due to oestrogenic actions correlated with reduced lipid peroxidation. ERβ activation may involve translocation of ERβ to the mitochondria and subsequent activation of direct or indirect mtDNA transcription. Differentially, ERβ but not ERα activation increased hippocampal expression of mtDNA-encoded COX I, a critical subunit of the electron transport chain terminal. Both ERα and ERβ activation increased nucDNA-encoded mitochondrial proteins including PDH subunit E1α, complex III core II subunit, COXIV, ATP synthase F1 subunit α and antioxidant proteins MnSOD and PrdxV. *In vitro*, SERM activation of either ERα or ERβ increased neuronal and glial respiratory capacity with activation of ERβ more involved with neuronal respiration. Recent reports from other groups indicate important anti-inflammatory roles of ERα in astrocytes (42) and ERβ in microglia (43–45), which may lead to new therapeutic targets. The reported findings in our study suggest that activation of both ERα and ERβ are differentially required to potentiate mitochondrial function in brain. As active components in hormone therapy, synthetically designed oestrogens as well as natural phyto-oestrogen cocktails can be tailored to improve brain mitochondrial endpoints.

Acknowledgments

This study was supported by grants from the National Institute of Aging (2R01AG032236 to R.D.B.).

Abbreviations

COX	cytochrome c oxidase
DPN	2,3-bis(4-hydroxyphenyl)propionitrile (diarylpropionitrile)
E2	17β-oestradiol (oestradiol)
ERK	extracellular signal-regulated kinase
MAPK	mitogen-activated protein kinases
MIB	mitochondrial isolation buffer
MnSOD	manganese superoxide dismutase
mtDNA	mitochondrial deoxyribonucleic acid
nucDNA	nuclear deoxyribonucleic acid
OVX	ovariectomy
PDH	pyruvate dehydrogenase
PPT	4,4′,4″-(4-propyl-[1H]-pyrazole-1,3,5-triyl)trisphenol (propylpyrazole triol)

PrdxV	peroxiredoxing V
RCR	respiratory control ratio
SERM	selective oestrogen receptor modulator

References

1. Nilsen J, Irwin RW, Gallaher TK, Brinton RD. Estradiol in vivo regulation of brain mitochondrial proteome. J Neurosci. 2007; 27(51):14069–77. [PubMed: 18094246]
2. Brinton RD. The healthy cell bias of estrogen action: mitochondrial bioenergetics and neurological implications. Trends in neurosciences. 2008; 31(10):529–37. [PubMed: 18774188]
3. Irwin RW, Yao J, Ahmed SS, Hamilton RT, Cadenas E, Brinton RD. Medroxyprogesterone acetate antagonizes estrogen up-regulation of brain mitochondrial function. Endocrinology. 2011; 152(2): 556–67. [PubMed: 21159850]
4. Irwin RW, Yao J, Hamilton RT, Cadenas E, Brinton RD, Nilsen J. Progesterone and estrogen regulate oxidative metabolism in brain mitochondria. Endocrinology. 2008; 149(6):3167–75. [PubMed: 18292191]
5. Bachmann GA. Menopausal vasomotor symptoms: a review of causes, effects and evidence-based treatment options. J Reprod Med. 2005; 50(3):155–65. [PubMed: 15841927]
6. Brinton RD. Estrogen-induced plasticity from cells to circuits: predictions for cognitive function. Trends Pharmacol Sci. 2009; 30(4):212–22. [PubMed: 19299024]
7. Brinton RD, Thompson RF, Foy MR, Baudry M, Wang J, Finch CE, Morgan TE, Pike CJ, Mack WJ, Stanczyk FZ, Nilsen J. Progesterone receptors: form and function in brain. Front Neuroendocrinol. 2008; 29(2):313–39. [PubMed: 18374402]
8. Mosconi L, Pupi A, De Leon MJ. Brain glucose hypometabolism and oxidative stress in preclinical Alzheimer's disease. Ann N Y Acad Sci. 2008; 1147:180–95. [PubMed: 19076441]
9. Beal MF. Mitochondria and neurodegeneration. Novartis Found Symp. 2007; 287:183–92. discussion 92–6. [PubMed: 18074639]
10. Reddy PH, Beal MF. Amyloid beta, mitochondrial dysfunction and synaptic damage: implications for cognitive decline in aging and Alzheimer's disease. Trends Mol Med. 2008; 14(2):45–53. [PubMed: 18218341]
11. Murphy AN, Bredesen DE, Cortopassi G, Wang E, Fiskum G. Bcl-2 potentiates the maximal calcium uptake capacity of neural cell mitochondria. Proc Natl Acad Sci U S A. 1996; 93(18): 9893–8. [PubMed: 8790427]
12. Nilsen J, Chen S, Irwin RW, Iwamoto S, Brinton RD. Estrogen protects neuronal cells from amyloid beta-induced apoptosis via regulation of mitochondrial proteins and function. BMC Neurosci. 2006; 774
13. Nilsen J, Diaz Brinton R. Mechanism of estrogen-mediated neuroprotection: regulation of mitochondrial calcium and Bcl-2 expression. Proc Natl Acad Sci U S A. 2003; 100(5):2842–7. [PubMed: 12604781]
14. Mannella P, Brinton RD. Estrogen receptor protein interaction with phosphatidylinositol 3-kinase leads to activation of phosphorylated Akt and extracellular signal-regulated kinase 1/2 in the same population of cortical neurons: a unified mechanism of estrogen action. J Neurosci. 2006; 26(37): 9439–47. [PubMed: 16971528]
15. Zhao L, Chen S, Ming Wang J, Brinton RD. 17beta-estradiol induces Ca2+ influx, dendritic and nuclear Ca2+ rise and subsequent cyclic AMP response element-binding protein activation in hippocampal neurons: a potential initiation mechanism for estrogen neurotrophism. Neuroscience. 2005; 132(2):299–311. [PubMed: 15802184]
16. Yao J, Irwin R, Chen S, Hamilton R, Cadenas E, Brinton RD. Ovarian hormone loss induces bioenergetic deficits and mitochondrial beta-amyloid. Neurobiol Aging. 2011
17. Yao J, Irwin RW, Zhao L, Nilsen J, Hamilton RT, Brinton RD. Mitochondrial bioenergetic deficit precedes Alzheimer's pathology in female mouse model of Alzheimer's disease. Proc Natl Acad Sci U S A. 2009; 106(34):14670–5. [PubMed: 19667196]

18. Shughrue PJ, Lane MV, Merchenthaler I. Comparative distribution of estrogen receptor-alpha and -beta mRNA in the rat central nervous system. J Comp Neurol. 1997; 388(4):507–25. [PubMed: 9388012]
19. Shughrue PJ, Merchenthaler I. Distribution of estrogen receptor beta immunoreactivity in the rat central nervous system. J Comp Neurol. 2001; 436(1):64–81. [PubMed: 11413547]
20. Zhao L, Wu TW, Brinton RD. Estrogen receptor subtypes alpha and beta contribute to neuroprotection and increased Bcl-2 expression in primary hippocampal neurons. Brain research. 2004; 1010(1–2):22–34. [PubMed: 15126114]
21. Zhao L, Mao Z, Brinton RD. A select combination of clinically relevant phytoestrogens enhances estrogen receptor beta-binding selectivity and neuroprotective activities in vitro and in vivo. Endocrinology. 2009; 150(2):770–83. [PubMed: 18818291]
22. Zhao L, Mao Z, Schneider LS, Brinton RD. Estrogen receptor beta-selective phytoestrogenic formulation prevents physical and neurological changes in a preclinical model of human menopause. Menopause. 2011
23. Mitterling KL, Spencer JL, Dziedzic N, Shenoy S, McCarthy K, Waters EM, McEwen BS, Milner TA. Cellular and subcellular localization of estrogen and progestin receptor immunoreactivities in the mouse hippocampus. J Comp Neurol. 2010; 518(14):2729–43. [PubMed: 20506473]
24. Stirone C, Duckles SP, Krause DN, Procaccio V. Estrogen increases mitochondrial efficiency and reduces oxidative stress in cerebral blood vessels. Molecular pharmacology. 2005; 68(4):959–65. [PubMed: 15994367]
25. Yang SH, Liu R, Perez EJ, Wen Y, Stevens SM Jr, Valencia T, Brun-Zinkernagel AM, Prokai L, Will Y, Dykens J, Koulen P, Simpkins JW. Mitochondrial localization of estrogen receptor beta. Proc Natl Acad Sci U S A. 2004; 101(12):4130–5. [PubMed: 15024130]
26. Milner TA, Lubbers LS, Alves SE, McEwen BS. Nuclear and extranuclear estrogen binding sites in the rat forebrain and autonomic medullary areas. Endocrinology. 2008; 149(7):3306–12. [PubMed: 18356271]
27. Chen JQ, Eshete M, Alworth WL, Yager JD. Binding of MCF-7 cell mitochondrial proteins and recombinant human estrogen receptors alpha and beta to human mitochondrial DNA estrogen response elements. J Cell Biochem. 2004; 93(2):358–73. [PubMed: 15368362]
28. Meyers MJ, Sun J, Carlson KE, Marriner GA, Katzenellenbogen BS, Katzenellenbogen JA. Estrogen receptor-beta potency-selective ligands: structure-activity relationship studies of diarylpropionitriles and their acetylene and polar analogues. J Med Chem. 2001; 44(24):4230–51. [PubMed: 11708925]
29. Stauffer SR, Coletta CJ, Tedesco R, Nishiguchi G, Carlson K, Sun J, Katzenellenbogen BS, Katzenellenbogen JA. Pyrazole ligands: structure-affinity/activity relationships and estrogen receptor-alpha-selective agonists. J Med Chem. 2000; 43(26):4934–47. [PubMed: 11150164]
30. Wang JM, Irwin RW, Brinton RD. Activation of estrogen receptor alpha increases and estrogen receptor beta decreases apolipoprotein E expression in hippocampus in vitro and in vivo. Proc Natl Acad Sci U S A. 2006; 103(45):16983–8. [PubMed: 17077142]
31. Han D, Williams E, Cadenas E. Mitochondrial respiratory chain-dependent generation of superoxide anion and its release into the intermembrane space. Biochem J. 2001; 353(Pt 2):411–6. [PubMed: 11139407]
32. Quesada A, Romeo HE, Micevych P. Distribution and localization patterns of estrogen receptor-beta and insulin-like growth factor-1 receptors in neurons and glial cells of the female rat substantia nigra: localization of ERbeta and IGF-1R in substantia nigra. J Comp Neurol. 2007; 503(1):198–208. [PubMed: 17480015]
33. Sheldahl LC, Shapiro RA, Bryant DN, Koerner IP, Dorsa DM. Estrogen induces rapid translocation of estrogen receptor beta, but not estrogen receptor alpha, to the neuronal plasma membrane. Neuroscience. 2008; 153(3):751–61. [PubMed: 18406537]
34. Duckles SP, Krause DN, Stirone C, Procaccio V. Estrogen and mitochondria: a new paradigm for vascular protection? Mol Interv. 2006; 6(1):26–35. [PubMed: 16507748]
35. Frasor J, Barnett DH, Danes JM, Hess R, Parlow AF, Katzenellenbogen BS. Response-specific and ligand dose-dependent modulation of estrogen receptor (ER) alpha activity by ERbeta in the uterus. Endocrinology. 2003; 144(7):3159–66. [PubMed: 12810572]

36. Lund TD, Rovis T, Chung WC, Handa RJ. Novel actions of estrogen receptor-beta on anxiety-related behaviors. Endocrinology. 2005; 146(2):797–807. [PubMed: 15514081]
37. Nilsen J, Brinton RD. Mitochondria as therapeutic targets of estrogen action in the central nervous system. Curr Drug Targets CNS Neurol Disord. 2004; 3(4):297–313. [PubMed: 15379606]
38. Ursini F, Maiorino M, Valente M, Ferri L, Gregolin C. Purification from pig liver of a protein which protects liposomes and biomembranes from peroxidative degradation and exhibits glutathione peroxidase activity on phosphatidylcholine hydroperoxides. Biochim Biophys Acta. 1982; 710(2):197–211. [PubMed: 7066358]
39. Lapointe J, Kimmins S, Maclaren LA, Bilodeau JF. Estrogen selectively up-regulates the phospholipid hydroperoxide glutathione peroxidase in the oviducts. Endocrinology. 2005; 146(6): 2583–92. [PubMed: 15746255]
40. Herst PM, Tan AS, Scarlett DJ, Berridge MV. Cell surface oxygen consumption by mitochondrial gene knockout cells. Biochim Biophys Acta. 2004; 1656(2–3):79–87. [PubMed: 15178469]
41. Wu M, Neilson A, Swift AL, Moran R, Tamagnine J, Parslow D, Armistead S, Lemire K, Orrell J, Teich J, Chomicz S, Ferrick DA. Multiparameter metabolic analysis reveals a close link between attenuated mitochondrial bioenergetic function and enhanced glycolysis dependency in human tumor cells. Am J Physiol Cell Physiol. 2007; 292(1):C125–36. [PubMed: 16971499]
42. Spence RD, Hamby ME, Umeda E, Itoh N, Du S, Wisdom AJ, Cao Y, Bondar G, Lam J, Ao Y, Sandoval F, Suriany S, Sofroniew MV, Voskuhl RR. Neuroprotection mediated through estrogen receptor-alpha in astrocytes. Proc Natl Acad Sci U S A. 2011; 108(21):8867–72. [PubMed: 21555578]
43. Saijo K, Collier JG, Li AC, Katzenellenbogen JA, Glass CK. An ADIOL-ERbeta-CtBP transrepression pathway negatively regulates microglia-mediated inflammation. Cell. 2011; 145(4):584–95. [PubMed: 21565615]
44. Leung YK, Ho SM. Estrogen receptor beta: switching to a new partner and escaping from estrogen. Sci Signal. 2011; 4(168):pe19. [PubMed: 21487104]
45. Leitman DC, Paruthiyil S, Vivar OI, Saunier EF, Herber CB, Cohen I, Tagliaferri M, Speed TP. Regulation of specific target genes and biological responses by estrogen receptor subtype agonists. Curr Opin Pharmacol. 2010; 10(6):629–36. [PubMed: 20951642]

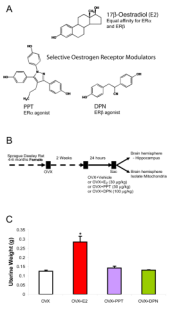

Figure 1. Chemical structures, experimental treatment paradigm, and uterine response in OVX rat model

A. Chemical structures of non-steroidal PPT and DPN in comparison with steroidal E2. These synthetic ligands have been used extensively as chemical tools to distinguish effects of ERα from ERβ in various research models. B. Ovaries were surgically removed from young adult female rats 2 wk before sc injection with E2, PPT, DPN or oil vehicle control. Twenty-four hours after the treatment, whole-brain mitochondria from the left hemisphere of the forebrain were isolated and subjected to a series of functional assessment experiments. The hippocampus was dissected from the right hemisphere of the forebrain and used to determine the expression of mitochondrial proteins. C. As a positive control, E2 induced an expected increase in uterine weight. At the doses used PPT and DPN did not change uterine weight suggesting that PPT and DPN had minimal oestrogenic side effects in the peripheral system (*=P<0.05 *vs*. OVX; n=4–5).

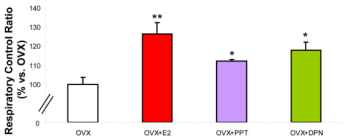

Figure 2. SERMs enhance brain mitochondrial respiratory activity

Mitochondrial oxygen consumption ± *in vivo* 17β-oestradiol (E2, 30 μg/kg), PPT (30 μg/kg), DPN (100 μg/kg) or corn oil vehicle control (OVX). Isolated mitochondria were energised by addition of L-malate (5 mM) and L-glutamate (5 mM) as substrates. ADP (410 μM) was added to stimulate state 3 respiration and rates were compared to ADP-depleted state 4, a surrogate for basal respiration. Data expressed as percent change in mitochondrial respiratory control ratio (RCR; state 3/state 4) relative to OVX. The data represents mean ± SEM of five separate experiments (*=$P<0.05$ as compared to OVX; $n=4–5$).

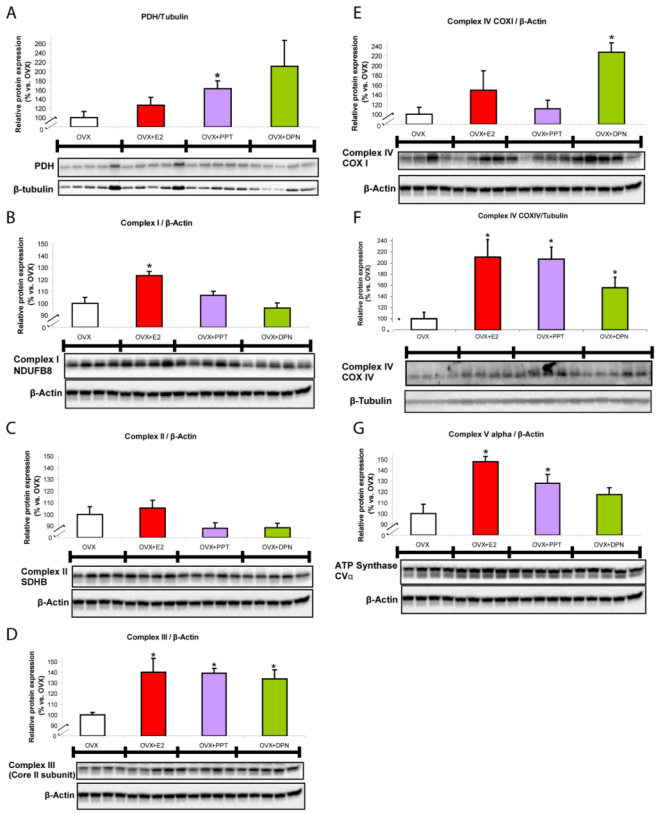

Figure 3. SERM-induced potentiation of protein profile of bioenergetics-related panel

Total protein was isolated from hippocampus following 24 h exposure to 17β-oestradiol (E2, 30 μg/kg), PPT (30 μg/kg), DPN (100 μg/kg) or corn oil vehicle control (OVX). All immunoblot data were normalised to β-tubulin or β-actin loading control and compared relative to OVX as 100%. Western blots were analysed to determine protein expression for: **A.** pyruvate dehydrogenase, subunit E1α of the PDH complex, the key enzyme linking glycolysis to the tricarboxylic acid cycle, responsible for catalysing the formation of acetyl-CoA and carbon dioxide from pyruvate within the mitochondria; **B.** complex I, subunit NDUFB8, accessory subunit of the mitochondrial membrane respiratory chain NADH dehydrogenase which functions in the transfer of electrons from NADH to the respiratory chain; **C.** complex II, subunit SDHB, one of the four subunits of succinate dehydrogenase located on the inner mitochondrial membrane and participates in both the tricarboxylic acid cycle and the respiratory chain; **D.** complex III, core II subunit, necessary for the formation of the complex, a component of the respiratory chain responsible for transferring electrons from coenzyme Q to cytochrome c; **E.** cytochrome c oxidase, subunit I (COXI), one of three mtDNA-encoded subunits of respiratory complex IV, located within the mitochondrial inner membrane and is the third and final enzyme of the electron transport chain of mitochondrial oxidative phosphorylation; **F.** cytochrome c oxidase, subunit IV (COXIV), one of ten nucDNA-encoded subunits of the enzyme complex IV; and **G.** complex V, subunit α, contained within the extramembraneous catalytic core of the complex that produces ATP from ADP in the presence of a proton gradient across the inner mitochondrial membrane. Panels B, C, D, E and G were blotted and analyzed simultaneously with a “mito-cocktail” antibody kit as described in the Methods section. Bars represent mean relative expression ± SEM from four to five animals per group (*=$P<0.05$ *vs*. OVX; $n=4–5$).

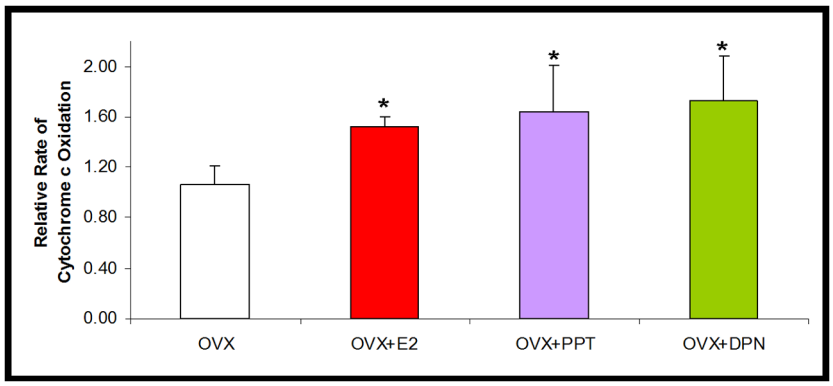

Figure 4. SERM-induced potentiation of cytochrome c oxidase activity

Relative rate of cytochrome c oxidation from isolated whole brain mitochondria ± *in vivo* 17β-oestradiol (E2, 30 μg/kg), PPT (30 μg/kg), DPN (100 μg/kg) or corn oil vehicle control (OVX). The bars represent mean ± SEM (*=$P<0.05$ *vs*. OVX; $n=4–5$).

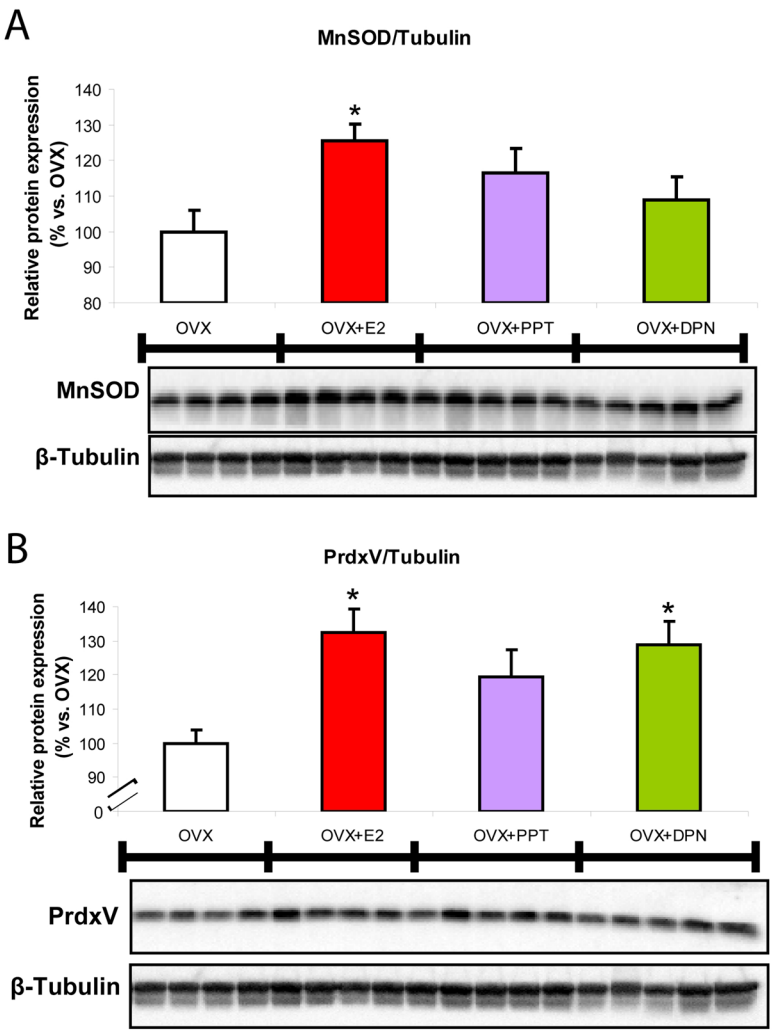

Figure 5. SERM-induced potentiation of the antioxidant capacity of brain mitochondria

A. Relative expression of antioxidant proteins peroxiredoxin V (PrdxV) and manganese superoxide dismutase (MnSOD) from isolated whole brain mitochondria ± *in vivo* 17β-oestradiol (E2, 30 μg/kg), PPT (30 μg/kg), DPN (100 μg/kg) or corn oil vehicle control (OVX). Immunoblot data were normalised to loading control and compared relative to OVX. Expression of the mitochondrial antioxidant proteins **A.** MnSOD in hippocampus and **B.** PrdxV in whole brain mitochondria were measured by Western blot analysis. In hippocampal lysates and isolated mitochondria, activation of ERβ stimulated expression of antioxidant proteins. The bars represent mean ± SEM (*=P<0.05 *vs*. OVX; n=4–5).

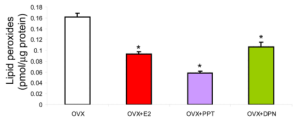

Figure 6. SERMs promoted clearance of ovariectomy-induced accumulation of lipid peroxidation

Whole brain mitochondria were isolated 24 h following *in vivo* exposure to 17β-oestradiol (E2, 30 μg/kg), PPT (30 μg/kg), DPN (100 μg/kg) or corn oil vehicle control (OVX). Lipid peroxides in purified brain mitochondria were measured using the leucomethylene blue assay. The bars represent mean ± SEM from 4 animals per group (*=P<0.05 as compared to OVX; n=4–5).

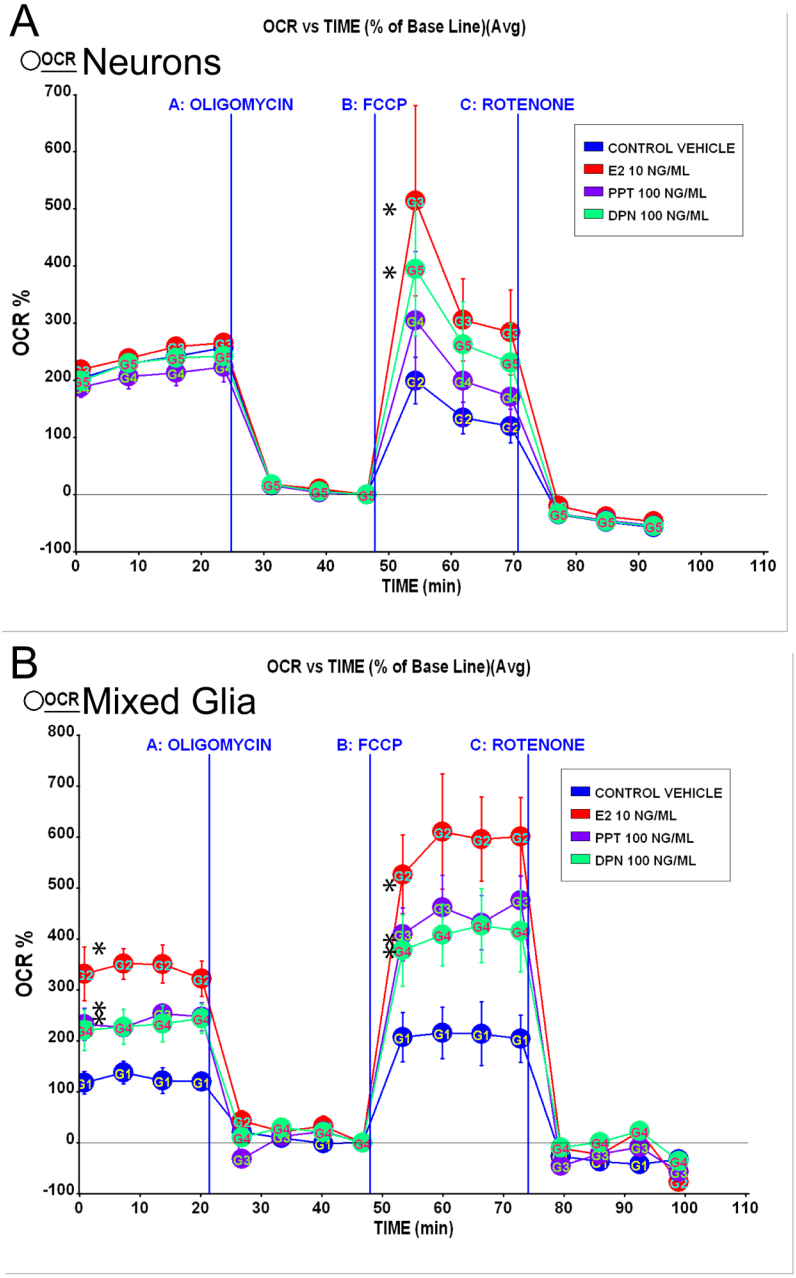

Figure 7. SERMs increased mitochondrial respiration *in vitro*

A. Primary rat embryonic (E18) neurones from hippocampus were cultured for 10 days in Neurobasal Media with B27 supplement and then treated with E2 (10 ng/ml), PPT (100 ng/ml), or DPN (100 ng/ml) or vehicle for 24 h prior to the experiment. Oxygen consumption rates (OCR) were determined using Seahorse XF-24 Metabolic Flux Analyzer. Vertical lines indicate time of addition of mitochondrial inhibitors A: oligomycin (1 μM), B: FCCP (1 μM) or C: rotenone (1 μM). OCR in primary neurones treated with E2 (10 ng/ml) and DPN (100 ng/ml) exhibited a greater magnitude of maximal mitochondrial respiratory capacity compared to vehicle (*=P<0.05 *vs*. vehicle; n=4). Primary rat embryonic (E18) mixed glia from hippocampus were cultured for 14 days in DMEM supplemented with 10% serum. **B.** Glial cells derived from primary rat embryonic (E18) hippocampus were cultured for 10

days before re-plating. Mixed glial cells were serum-starved 4 h then treated with E2 (10 ng/ml), PPT (100 ng/ml), DPN (100 ng/ml) or vehicle for 24 h prior to the experiment. Vertical lines indicate time of addition of mitochondrial inhibitors A: oligomycin (1 μM), B: FCCP (1 μM) or C: rotenone (1 μM). OCR in primary glia treated with E2 (10 ng/ml), PPT (100 ng/ml), or DPN (100 ng/ml) displayed greater basal respiration and increased maximal mitochondrial respiratory capacity compared to vehicle (*=$P<0.05$ *vs*. vehicle; $n=4$).

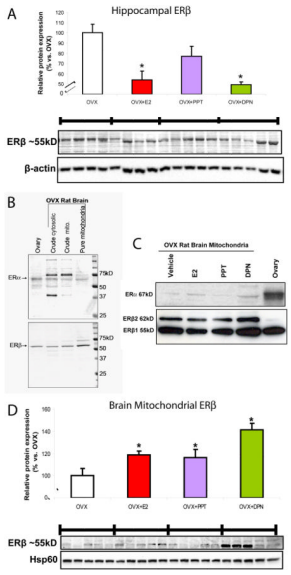

Figure 8. Detection of ERα and ERβ in purified brain mitochondria and ERβ expression patterns following SERM-treatment

Total protein was isolated from hippocampus or whole brain purified mitochondria 24 h following *in vivo* exposure to 17β-oestradiol (E2, 30 μg/kg), PPT (30 μg/kg), DPN (100 μg/kg) or corn oil vehicle control (OVX). **A.** Hippocampal ERβ (antibody PA1-310b; 1:500) expression was determined by Western blot analysis. Expression of immunoblot data were normalised to β-actin loading control and compared relative to OVX as 100%. Bars represent mean relative expression ± SEM (*=P<0.05 *vs*. OVX; n=4–5). **B**. Existence of brain mitochondrial ERα (6F11; 1:50) and ERβ (H-150; 1:500) was verified by Western blot of OVX rat brain mitochondria. Crude cytosolic and crude mitochondrial fractions from the purification procedure demonstrated the enriched localization of ER-immunoreactivity to highly purified mitochondria. Blots were intentionally overexposed to demonstrate that non-specific protein binding is diminished as mitochondrial purity increased. ERα (67 kD), ERβ1 (55 kD), and ERβ2 (62 kD) were concentrated as immunoreactive bands in the mitochondrial fraction. Proteins extracted from rat ovary lysate confirmed ER antibody specificity at the appropriate molecular size. **C.** Upper blot: representative of mitochondrial-associated ERα (67 kD) detected with 6F11 antibody (not quantified). We observed that compared to ovary lysate control, overall, mitochondrial associated ERα was much less abundant, equal loading, 20μg protein/lane. Lower blot: antibody H-150 detected mitochondrial ERβ1 (55 kD), and ERβ2 (62 kD) expression determined by Western blot (not quantified). **D.** Quantified immunodetection of ERβ1 (55 kD). Mitochondrial ERβ (antibody PA1-310b; 1:500) was determined by Western blot analysis. Immunoblot data normalised to Hsp60 loading control and treatment groups compared relative to OVX as 100%. Twnety-four hours following DPN treatment (100 μg/kg), three of the five purified rat brain mitochondrial samples showed intense ERβ immunoreactivity. Bars represent mean relative expression ± SEM from five animals per group (*=P<0.05 *vs*. OVX; n=5).